This is a repository copy of *Mechanical properties of soda-lime-silica glasses with varying alkaline earth contents*.

White Rose Research Online URL for this paper:
http://eprints.whiterose.ac.uk/95393/

Version: Accepted Version

Article:
Kilinc, E. and Hand, R.J. orcid.org/0000-0002-5556-5821 (2015) Mechanical properties of soda-lime-silica glasses with varying alkaline earth contents. Journal of Non-Crystalline Solids, 429. pp. 190-197. ISSN 0022-3093

https://doi.org/10.1016/j.jnoncrysol.2015.08.013

Article available under the terms of the CC-BY-NC-ND licence
(https://creativecommons.org/licenses/by-nc-nd/4.0/)

Reuse
This article is distributed under the terms of the Creative Commons Attribution-NonCommercial-NoDerivs (CC BY-NC-ND) licence. This licence only allows you to download this work and share it with others as long as you credit the authors, but you can't change the article in any way or use it commercially. More information and the full terms of the licence here: https://creativecommons.org/licenses/

Takedown
If you consider content in White Rose Research Online to be in breach of UK law, please notify us by emailing eprints@whiterose.ac.uk including the URL of the record and the reason for the withdrawal request.

eprints@whiterose.ac.uk
https://eprints.whiterose.ac.uk/

Mechanical properties of soda-lime-silica glasses with varying alkaline earth contents

Erhan Kilinc & Russell J Hand
Department of Materials Science & Engineering, University of Sheffield, Sir Robert Hadfield Building, Mappin Street, Sheffield, S1 3JD, UK

Abstract

The effects of varying the alkaline earth oxide content of three series of soda-lime-silica glasses with the general formulae $13.5Na_2O{\cdot}xMgO{\cdot}10CaO{\cdot}1.5Al_2O_3{\cdot}(75 - x)SiO_2$ (mol%) where x = 0, 1, 2, 3, 4, 5, 6, 7; $13.5Na_2O{\cdot}3MgO{\cdot}(7 + y)CaO{\cdot}1.5Al_2O_3{\cdot}(75 - y)SiO_2$ (mol%) where y = 0, 1, 2, 3, 4, 5, 6, 7 and $13.5Na_2O{\cdot}zMgO{\cdot}(13 - z)CaO{\cdot}1.5Al_2O_3{\cdot}72SiO_2$ (mol%) where z = 1, 3, 5, 7, 9, 11 have been examined. Raman spectroscopy and nuclear magnetic resonance (NMR) spectroscopy have been used to assess network connectivity. In the first two glass series network connectivity decreases with increasing alkaline earth addition whereas in the third series connectivity tends to be greater for the more magnesia rich glasses suggesting that magnesia does have a different effect to lime on network connectivity, but only when magnesia is the dominant alkaline earth species. Fracture toughness has been measured using bend testing, which avoids many of the questions raised by the widely used indentation technique. Moduli have been assessed using acoustic means. It was found that the mechanical properties tend to decrease with increasing network connectivity for all three glass series. For the $MgO\text{-}SiO_2$ series and $CaO\text{-}SiO_2$ glasses increasing the alkaline earth content at the expense of the silica content resulted in increased network depolymerisation, whereas for the MgO-CaO series when MgO became the dominant alkaline earth species, network depolymerisation was reduced. Thus while MgO and CaO both act as network modifiers when more CaO than MgO is present in soda-lime-silica glasses, a difference in behaviour is seen with magnesia rich soda-magnesia-silica glasses. In contradiction to previous data no significant advantage of replacing CaO by MgO is observed. In addition it appears that the glasses with the lowest fracture toughness values may be more resilient to contact damage than those with the higher fracture toughness values.

1. Introduction

There is a significant interest in reducing the weight and hence thickness of glass products in a number of applications[1] and this will require intrinsically stronger glass products[2]. Whilst very thin high strength glasses, such as Corning Gorilla® glass, are routinely produced for display applications, the processes used are expensive and not suited to bulk glass applications such as containers and glassware. Bulk glass production is based on a limited range of soda-lime-silica (SLS) compositions with 90% of all glass manufactured globally having this type of composition[3], albeit containing a range of other minor components. Even within a restricted compositional range some variation of mechanical properties with composition is to be expected and a number of authors have reported studies looking at such effects[1,2,4,5,6,7]. Most of the reported work is largely empirical, although Makashima and Mackenzie suggested an essentially linear model for calculating how the elastic moduli of a range of silicate and borate glasses vary with composition in the 1970s[8,9]. The more recent collection of Poisson's ratio data by Rouxel indicates that, at least some aspects, of this model are incorrect as the linear variation of Poisson's ratio with packing fraction predicted by the model was not observed[10].

Other work has given indications of non-linear variations in mechanical properties when one alkali is exchanged for another[4,5,7] with reduced ionic mobility in mixed alkali glasses apparently resulting in reduced plastic flow in indentation. In addition the literature indicates that alkaline earths also play an important role in controlling the mechanical properties. Thus the results of Deriano et al.[7] and Hand and Tadjiev[2] indicate that increased fracture toughness values may be obtained by increasing the MgO content, while reducing the CaO content at constant SiO_2 and Na_2O concentrations. The ionic radius and coordination number of Mg are smaller than those of Ca and thus substitution of MgO for CaO gives higher molar volumes which it is suggested may explain the increase in fracture toughness[4]. Due the small size of Mg there is also debate as to whether magnesium acts entirely as a network modifier[11] although the NMR results of Deriano et al.[6] indicate that, at least in the compositions they studied, that MgO does behave as a network modifier in soda-lime-silica glasses. Alternatively the presence of smaller and mobile alkaline earth ions (Mg^{2+}) rather than larger less mobile alkaline earth ions (Ca^{2+}, Sr^{2+} or Ba^{2+}) might increase plastic flow, and consequently fracture toughness as observed for mixed alkali silicate glasses[7].

Another compositional factor that is expected to affect the mechanical properties of silicate glasses is changes in network connectivity. Thus increasing SiO_2 at the expense of alkali or

alkaline earth oxides, thereby increasing the network connectivity is reported to enhance indentation fracture toughness[2]. Overall therefore the mechanical properties of silicate glasses do vary with composition and it would be beneficial to identify glasses with high fracture toughness values, as increased fracture toughness values can reasonably be expected to lead to increased strengths, although this does, of course, depend on the size of the strength controlling flaws that are present in the glass.

Hence in the current study, the effects of replacing SiO_2 with MgO or CaO, or replacing MgO by CaO with fixed SiO_2 content on the mechanical properties of glasses based on a simplified commercial soda-lime-silica glass composition are investigated. As well as measuring mechanical properties, Raman, infra-red and nuclear magnetic resonance (^{29}Si NMR) spectroscopies have been used to gain insight into the structural basis for the measured variations in the mechanical properties of the glasses.

2. Experimental

2.1. Sample preparation

Three series of glasses (MgO-SiO_2, CaO-SiO_2 & MgO-CaO series) have been produced. In the MgO-SiO_2 series the MgO:SiO_2 ratio was modified whilst in the CaO-SiO_2 series the CaO:SiO_2 ratio was modified. In both cases the concentration of all other constituents remained constant. In the MgO-CaO series the MgO:CaO has been modified whilst the concentration of all other constituents remained constant. The general formula of the MgO-SiO_2 series was $13.5Na_2O \cdot xMgO \cdot 10CaO \cdot 1.5Al_2O_3 \cdot (75 - x)SiO_2$ (mol%) where x = 0, 1, 2, 3, 4, 5, 6, 7; that of the CaO-SiO_2 series was $13.5Na_2O \cdot 3MgO \cdot (7 + y)CaO \cdot 1.5Al_2O_3 \cdot (75 - y)SiO_2$ (mol%) where y = 0, 1, 2, 3, 4, 5, 6, 7 and that of the MgO-CaO series was $13.5Na_2O \cdot zMgO \cdot (13 - z)CaO \cdot 1.5Al_2O_3 \cdot 72SiO_2$ (mol%) where z = 1, 3, 5, 7, 9, 11. Glass codes are of the form $M_pC_qS_r$ where p, q and r are the batched molar contents of MgO, CaO and SiO_2 respectively.

Batches to produce 300 g of glass were batched using SiO_2 (99.5%), Na_2CO_3 (99.1%), $CaCO_3$ (99.3%), (all from Glassworks Services), Na_2SO_4 (from Acros Organics), $4MgCO_3 \cdot Mg(OH)_2 \cdot 5H_2O$ and $Al(OH)_3$ (both from Fisher Scientific). In most compositions, ~3 mol% of the total Na_2O was supplied using Na_2SO_4 as a refining agent. The well mixed batch was transferred to a zirconia stabilized platinum crucible and heated to 1450 ºC in an

electric furnace for a total of 5 hours. After allowing one hour to achieve a batch free melt a Pt stirrer was inserted into the melt and the melt was stirred during the remaining 4 hours of melting during which refining and homogenization occurred. Finally the molten glass was cast into a pre-heated stainless steel mould. After demoulding the still hot glass was transferred to an annealing furnace, where it was held at 560°C for one hour and then cooled to room temperature at a rate of 1°C/min.

~ 20×20×3 mm samples were cut from the annealed glass bar on Buehler ISOMET 5000. The samples were successively ground using MetPrep 120, 240, 400, 600, 800 and 1200 SiC grinding papers and finally successively polished using MetPrep 6 μm (oil based), 3 μm (oil based) and 1 μm (water based) diamond suspensions to achieve a mirror like finish. To remove residual stresses arising from the cutting, grinding and polishing the samples were re-annealed by heating to the annealing temperature at 1°C/min, holding for one hour and then cooling down to room temperature at a rate of 1°C/min. A polariscope was used to check that the residual stresses had been removed by the re-annealing.

2.2 Chemical and physical measurements

The chemical compositions of the as-produced glasses were measured by XRF at Glass Technology Services, Sheffield. Density was measured using Archimedes' principle with distilled water as the immersion medium on a Mettler Toledo density balance. Differential thermal analysis was used to measure the glass transition temperatures of the glasses produced glasses. A Perkin Elmer Pyris 1 TGA was used. Fine powder samples were heated up to 1000 °C at a heating rate of 10 °C/min, cooled down to room temperature at the same rate and then re-heated up to 1000 ºC again at 10 ºC/min. The glass transition temperatures were obtained from the second heating curve using the in-built Perkin-Elmer software.

2.3 Structural analysis

Structural analysis was primarily conducted using Raman spectroscopy. Some samples were also studied using magic angle spinning nuclear magnetic resonance (MAS-NMR) to confirm the data obtained from the Raman analysis.

Raman spectra were obtained using a Renishaw InVia Raman Spectrometer. Before each test the instrument was calibrated using a Si wafer reference standard. Excitation of the polished and annealed glass surfaces was undertaken using a 514.5 nm laser at a laser power of 20 mW. The laser beam was magnified 50× and focused at a depth just beneath the polished surface. The exposure and acquisition times were both 10 s. The raw data were transferred to Labspec software and a baseline fitted by linearly connecting four points where the spectra goes to zero following the method of Colomban et al[12]. This baseline was subtracted from the spectra which were then exported to Peakfitv4.12 software in order to calculate the area under the bands of interest.

^{29}Si NMR analysis of selected samples was undertaken using ^{29}Si NMR analysis was undertaken using a Varian Unity Inova 300. 0.5-1.0 grams of powdered samples were tested at the EPSRC National Solid State NMR service at the University of Durham, UK. The chemical shifts of the ^{29}Si NMR spectra of the samples are referenced to tetramethylsilane (TMS). Pulse angle, acquisition time and resonance frequency were set to 45°, 40.00 ms and 59.557 MHz respectively.

2.4 Mechanical property measurements

Hardness was assessed using Vickers indentation. The polished surfaces were indented with a load of 9.81 N for 20 seconds using a Mitutoyo Vickers indenter. The number of indentations made on each composition was ~10. The hardness was calculated using

$$H_V = \frac{1.854P}{d^2} \quad (1)$$

where d is the length of the indent diagonals.

Fracture toughness of the glasses was measured using bend testing with a controlled defect introduced via Knoop indentation in accordance with the BS EN ISO 18756: 2005[13] standard. The samples were bars 3.5 × 4.0 × 46 mm on average, cut from the as cast bulk glass blocks and the side to be placed in tension successively ground to a 600 grit finish. In order to prevent possible notch tip blunting, samples were annealed, prior to introducing the Knoop indentation at the centre of the 46 × 4.0 mm face using a 2 kg (19.62 N) load. The indentation process can introduce further residual stresses as well as lateral cracks, that might modify the stress intensity at the crack tip and consequently give erroneous fracture toughness

values[14,15,16,17]. The standard therefore recommends grinding the indented surface of the specimen in order to remove the residual stress zone, however grinding can also introduce extra residual stresses in glasses[16]. Hence in order to clarify the effect of residual stress on the fracture toughness, specimens were prepared both 'as-indented' and 'ground', where in line with the standard, residual stresses due to the impression were minimized by gently grinding 20-25 μm from the specimen surface using 600 grit grinding paper in a direction perpendicular to the Knoop indent long diagonal. No significant differences were seen in the results obtained with the two conditions.

A four point bend fixture with articulating rollers was used with inner and outer spans set to 20 mm and 40 mm, respectively. The fixture was mounted on a Hounsfield TX0038 universal testing machine. In order to minimize environmental effect whilst the specimens are bent, the pre-crack was filled with silicone oil and approach speed and crosshead speed were set to 0.25 and 0.5 mm/min, respectively. A total of 177 specimens were prepared across all the compositions studied and 123 specimens fractured properly from the controlled defect and therefore analysed further. The fracture toughness was calculated using

$$K_{Ic} = Y_{max} \frac{3PS}{BW^2} \sqrt{a} \qquad (2)$$

where P is load, Y_{max} is the maximum stress intensity factor (see appendix for details), S is the span between the inner and outer loading points, B is plate thickness, W is plate width and a is flaw depth.

The geometry of the semi–elliptical crack causing fracture was assessed from the fracture surfaces using the Buehler multi focus tool on a Nikon Eclipse LV150 microscope equipped with Buehler OMNIMET 9.5 software. If the geometry of the characterized pre-crack did not meet the requirements of Annex B in BS EN ISO 18756: 2005[13], the result was rejected.

Brittleness was obtained from the measured hardness and fracture toughness values using

$$B = \frac{H_V}{K_{Ic}}. \qquad (3)$$

Elastic moduli of the produced glasses were obtained by measuring the longitudinal (V_L) and transverse (V_T) ultrasonic wave velocities using an Olympus Epoch 6000. The shear modulus, G, was obtained using

$$G = \rho V_T^2, \tag{4}$$

where ρ is density, and Young's modulus, E, was obtained using

$$E = \rho V_T^2 \frac{\left(3V_L^2 - 4V_T^2\right)}{\left(V_L^2 - V_T^2\right)}. \tag{5}$$

To minimise the cumulative error Poisson's ratio and bulk modulus were also obtained from the wave velocities using

$$\nu = \frac{\left(V_L^2 - 2V_T^2\right)}{2\left(V_L^2 - V_T^2\right)} \tag{6}$$

and

$$K = \rho \frac{3V_L^2 - 4V_T^2}{3} \tag{7}$$

respectively.

3. Results and Discussion

3.1. Chemical and physical measurements

The analysed glass compositions are given in table 1. Although there is generally good agreement between the batched and measured values there are small systematic differences. In particular the magnesia values tend to be lower than batched, whereas the lime ones tend to be slightly higher. In addition the soda values tend to be slightly low for the CaO-SiO_2 series and the alumina tends to be low for the MgO-CaO series. Iron is also found as an impurity in all of the glasses and traces of Zn were found in some compositions. Overall all of the glasses were deemed to be close enough to the batched composition to be used in the rest of the study.

Table 1. Analysed glass compositions (mol%); XRF data normalised to give mol%. Batched compositions were $13.5Na_2O \cdot xMgO \cdot 10CaO \cdot 1.5Al_2O_3 \cdot (75 - x)SiO_2$ (mol%) where x = 0, 1, 2, 3, 4, 5, 6, 7 for the MgO-SiO_2 series; $13.5Na_2O \cdot 3MgO \cdot (7 + y)CaO \cdot 1.5Al_2O_3 \cdot (75 - y)SiO_2$ (mol%) where y = 0, 1, 2, 3, 4, 5, 6, 7 for the CaO-SiO_2 series and $13.5Na_2O \cdot zMgO \cdot (13 -$

z)$CaO \cdot 1.5Al_2O_3 \cdot 72SiO_2$ (mol%) where z = 1, 3, 5, 7, 9, 11 for MgO-CaO series. Glass codes are of the form $M_pC_qS_r$ where p, q and r are the batched molar contents of MgO, CaO and SiO_2 respectively. For convenience glass $M_3C_{10}S_{72}$ appears in all 3 datasets.

Glass code	**SiO_2**	**Na_2O**	**CaO**	**MgO**	**Al_2O_3**	**Fe_2O_3**	**ZnO**	**SO_3**	**Σ[RO] /[SiO_2]**	**[MgO] /Σ[RO]**
$M_0C_{10}S_{75}$	74.87	13.28	10.33	0.00	1.49	0.03	0.00	0.00	0.138	0.000
$M_1C_{10}S_{74}$	74.07	13.51	9.89	1.00	1.52	0.03	0.00	0.00	0.147	0.092
$M_2C_{10}S_{73}$	73.01	13.31	10.29	1.88	1.48	0.04	0.00	0.00	0.167	0.155
$M_3C_{10}S_{72}$	72.20	12.88	10.40	2.98	1.52	0.03	0.00	0.00	0.185	0.223
$M_4C_{10}S_{71}$	70.67	13.43	10.39	3.82	1.52	0.03	0.00	0.15	0.201	0.269
$M_5C_{10}S_{70}$	69.65	13.76	10.23	4.82	1.51	0.04	0.00	0.00	0.216	0.320
$M_6C_{10}S_{69}$	68.93	13.34	10.33	5.80	1.54	0.03	0.02	0.00	0.234	0.360
$M_7C_{10}S_{68}$	68.04	13.29	10.39	6.76	1.45	0.04	0.01	0.00	0.252	0.394
$M_3C_7S_{75}$	75.54	12.80	7.24	2.89	1.45	0.03	0.00	0.00	0.134	0.285
$M_3C_8S_{74}$	73.82	13.58	8.25	2.83	1.49	0.01	0.00	0.00	0.150	0.256
$M_3C_9S_{73}$	73.11	13.09	9.31	2.88	1.54	0.03	0.03	0.00	0.167	0.236
$M_3C_{10}S_{72}$	72.20	12.88	10.40	2.98	1.52	0.03	0.00	0.00	0.185	0.223
$M_3C_{11}S_{71}$	71.00	13.06	11.43	2.96	1.51	0.03	0.00	0.00	0.203	0.206
$M_3C_{12}S_{70}$	70.16	13.15	12.27	2.87	1.49	0.03	0.00	0.00	0.216	0.190
$M_3C_{13}S_{69}$	68.99	13.24	13.34	2.87	1.52	0.03	0.00	0.00	0.235	0.177
$M_3C_{14}S_{68}$	68.05	13.23	14.34	2.87	1.48	0.05	0.00	0.00	0.253	0.167
$M_1C_{12}S_{72}$	72.08	13.50	12.13	1.00	1.26	0.03	0.00	0.00	0.182	0.076
$M_3C_{10}S_{72}$	72.20	12.88	10.40	2.98	1.52	0.03	0.00	0.00	0.185	0.223
$M_5C_8S_{72}$	72.75	13.07	8.20	4.76	1.18	0.04	0.00	0.00	0.178	0.367
$M_7C_6S_{72}$	73.04	12.91	6.19	6.66	1.17	0.03	0.00	0.00	0.176	0.518
$M_9C_4S_{72}$	72.60	13.13	4.12	8.89	1.22	0.04	0.00	0.00	0.179	0.683
$M_{11}C_2S_{72}$	72.12	13.53	2.03	11.01	1.26	0.03	0.01	0.00	0.181	0.844

3.2. Structural analysis

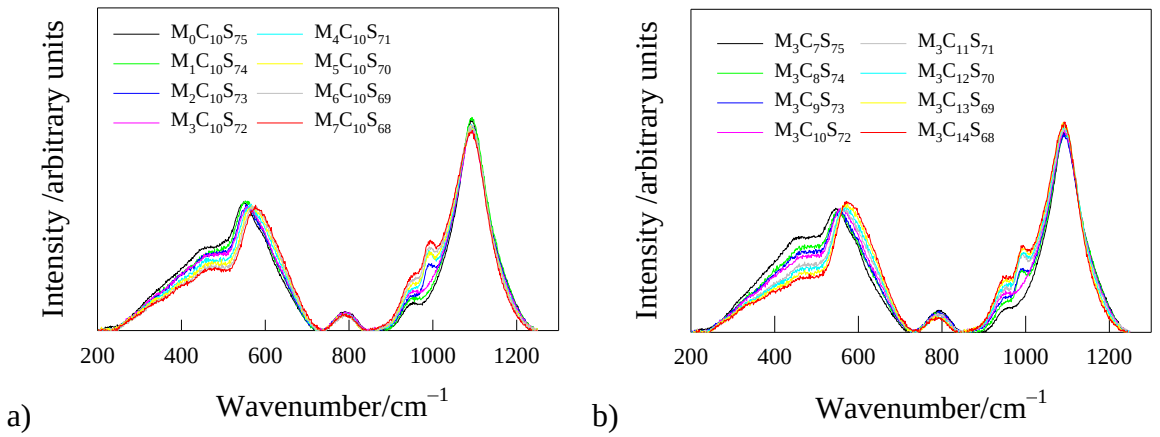

Figure 1: Normalised Raman spectra for a) the $MgO\text{-}SiO_2$ series and b) the $CaO\text{-}SiO_2$ series glasses

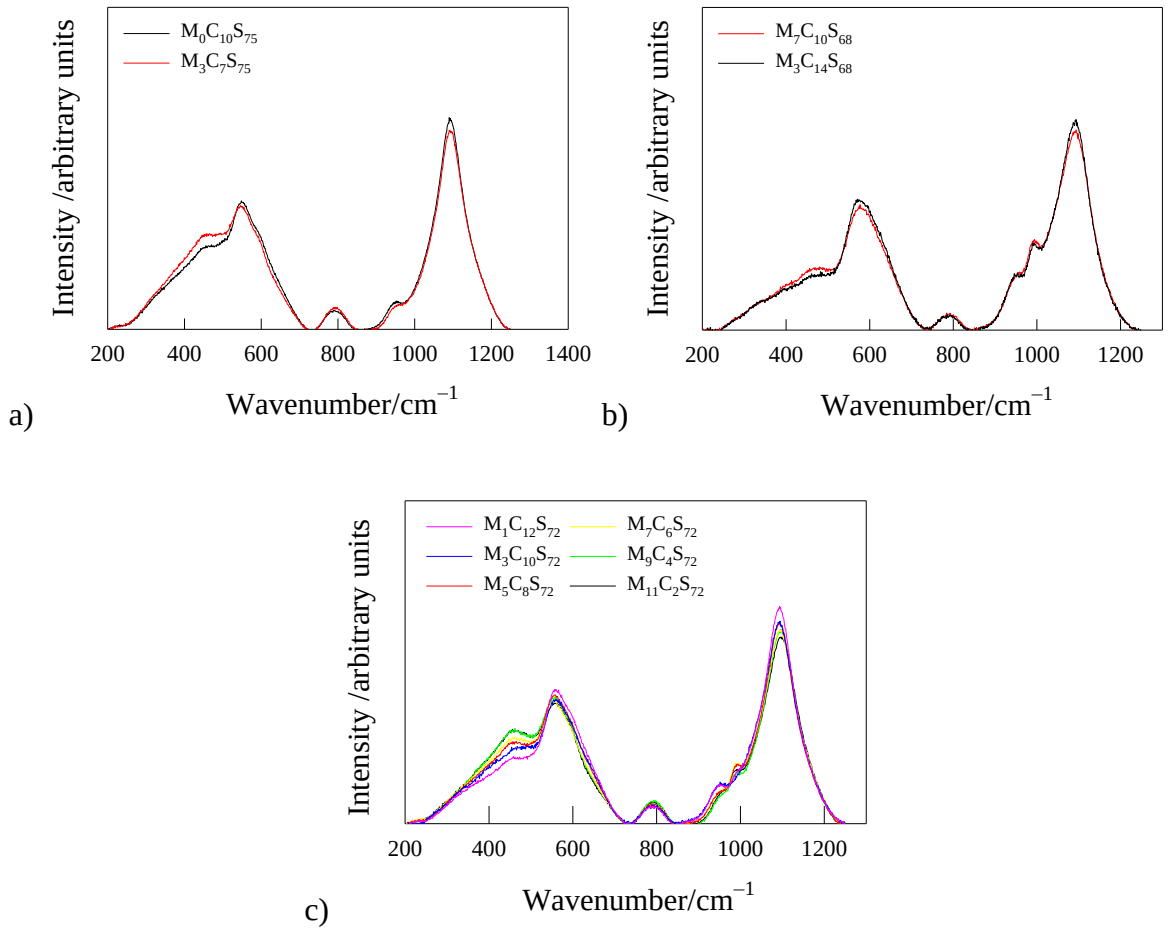

Figure 2: Normalised Raman spectra for a) the lowest alkali oxide earth content glasses ($M_0C_{10}S_{75}$ and $M_3C_7S_{75}$) in the $MgO\text{-}SiO_2$ and $CaO\text{-}SiO_2$ series, b) the highest alkali earth

oxide content glasses ($M_7C_{10}S_{68}$ and $M_3C_{14}S_{68}$) in the MgO-SiO_2 and CaO-SiO_2 series and c) the MgO-CaO series

Figure 1 shows Raman spectra for both series of glasses studied here; the spectra have been normalised to the same total area under the curve after baseline subtraction following the method of Le Losq et al[18]. It is clear that all of the spectra exhibit the same major 3 features namely a broad band between ~300 and 700 cm^{-1} (referred to in the following as region A), which is associated with bending modes of silica tetrahedra[19,20,21,22], a small band centred on ~785 cm^{-1} (referred to in the following as region B) and a broad band between ~900 and 1300 cm^{-1} (referred to in the following as region C). Regions B and C are associated with stretching modes of silica tetrahedra with the former being due to silicon motion[23] in Q^0 units[19] and the latter to stretching motions involving Q^1, Q^2, Q^3 and Q^4 units[19,20,22]. It can also be seen that the shoulder at ~500 cm^{-1} reduces as the MgO:SiO_2 or CaO:SiO_2 ratio increases (see figures 1a and 1b); and this shoulder increases as the MgO:CaO ratio increases (see figure 2c). The presence of this feature is associated with 5, 6 or higher membered silica rings and this suggests that the average ring size is smaller in the glasses with lower silica or ones containing larger amounts of CaO[18]. The shoulder at ~ 1000 cm^{-1} increases as the alkaline earth content increases for both series of glasses indicating that the amount of non-bridging oxygen increases as SiO_2 is replaced with either MgO or CaO[24]. In addition as the total alkaline earth oxide content increases the position of the peak at ~ 600 cm^{-1} shifts to higher wavenumbers. McMillan[24] has suggested that in silicate glasses, a reduction in the degree of polymerization and in SiO_2 content shifts the position of the 400-700 cm^{-1} band to higher frequencies. Overall these changes indicate that in both series there is increasing depolymerisation of the glass network as the alkaline earth oxide content increases[19].

The feature at 990 cm^{-1} is believed to be related to dissolved sulphur which will originate from the Na_2SO_4 used for fining[25], although no sulphur was detected in most of the XRF test results for the glasses produced here. However, Na_2SO_4 was not added to the $M_7C_{10}S_{68}$ batch and this shoulder did not appear in the spectra of $M_7C_{10}S_{68}$ supporting the assignment of this band to dissolved sulphur.

Many studies have attempted to decompose and calculate the contributions from different Q^n species to the peak in region C. However the fabricated glasses here contain a constant amount of Al_2O_3 (~1.5 mol%) which can be expected to behave as a network former, due to the presence of sufficient Na_2O to provide the necessary charge balance. Due to the

complexities of quantification of Q^4(Si) and Q^4(Al) species in this spectral range[25] detailed Q species quantification has therefore not been undertaken here. Instead the Raman polymerization index which is given by the ratio of the intensity of region C to that of the region A has been used to gain insight into the degree of polymerization, with a higher value of this index indicating a greater degree of connectivity[26,27]. To obtain the total area under the peaks in region A and region C the spectra in these regions were fitted by 4 or 5 Gaussian bands as required. For the spectra which contain a sulphate shoulder at 990 cm^{-1} the relevant Gaussian was then excluded from the subsequent area and polymerization index calculations. The degree of polymerization, as measured by the Raman polymerization index, decreases as a function of [MgO + CaO]/[SiO_2] increases (see Figure 3a). Figure 3b shows that a higher MgO content for a given SiO_2 tends to give a higher value of the Raman polymerization index. Although in principle the data in figure 3a can be replotted in terms of the MgO / (MgO + CaO) ratio no further insight is gained as the variation of alkaline earth to silica content tends to dominate the observed behaviour of the polymerization index for the MgO-SiO_2 and CaO-SiO_2 series glasses. Figure 3b does however indicate that there are some changes in network polymerization as MgO is substituted by CaO when all other components are fixed.

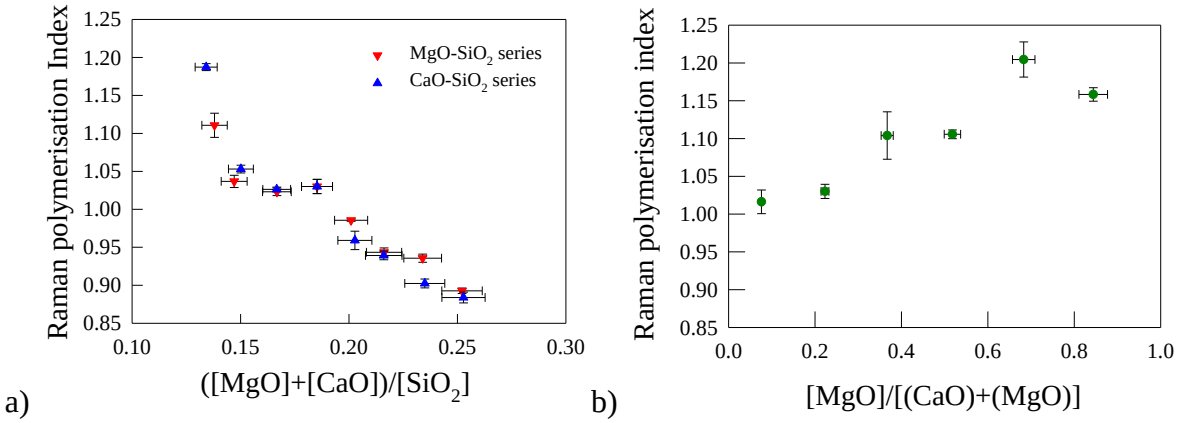

Figure 3: Raman polymerisation index for a) the MgO-SiO_2 series and CaO-SiO_2 series glasses as a function of total alkaline earth content divided by silica content and b) for the MgO-CaO series as a function of MgO content divided by total alkaline earth content

^{29}Si NMR spectroscopy of selected samples from the MgO-SiO_2 and CaO-SiO_2 series glasses was undertaken to provide an independent measure of the Q^n species present in a selection of the glasses studied here and the results are shown in figures 4a and 4b. It can be seen that as either MgO or CaO are substituted for SiO_2 the same general changes in the spectra occur. As

shown by two examples in figure 5 all of the NMR traces can be fitted with just 2 Gaussians, one at chemical shift of approximately –105 ppm indicating the presence of Q^4 silicate units and the other at a chemical shift of approximately –92 ppm indicating the presence of Q^3 silicate units[28,29]. NMR gives no evidence of Q^2, Q^1 or Q^0 species being present in these glasses.

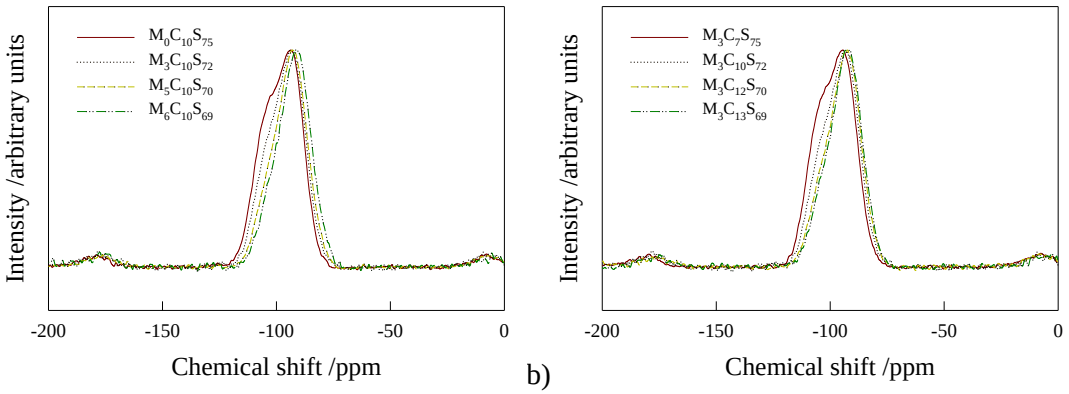

Figure 4. ^{29}Si NMR spectra for selected glasses from a) the MgO-SiO_2 glass series and b) the CaO-SiO_2 glass series.

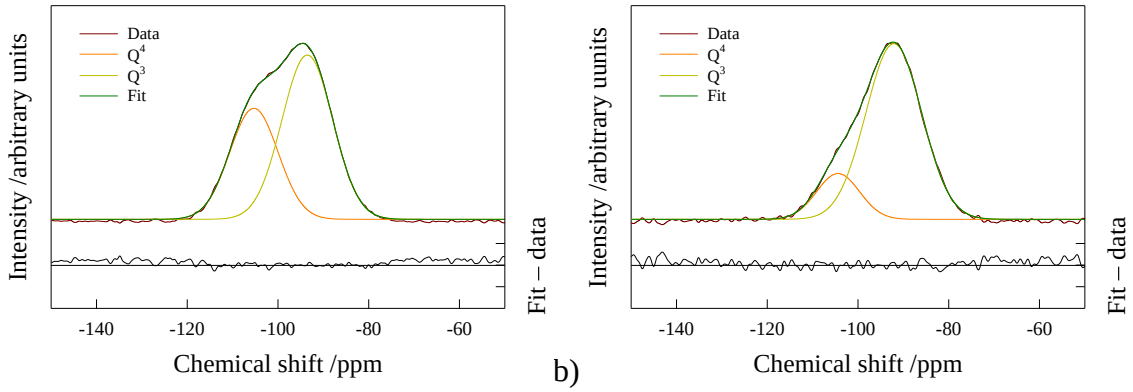

Figure 5. Example deconvolutions of the ^{29}Si NMR spectra shown in figure 3 a) $M_3C_7S_{75}$ glass and b) $M_3C_{13}S_{69}$ glass.

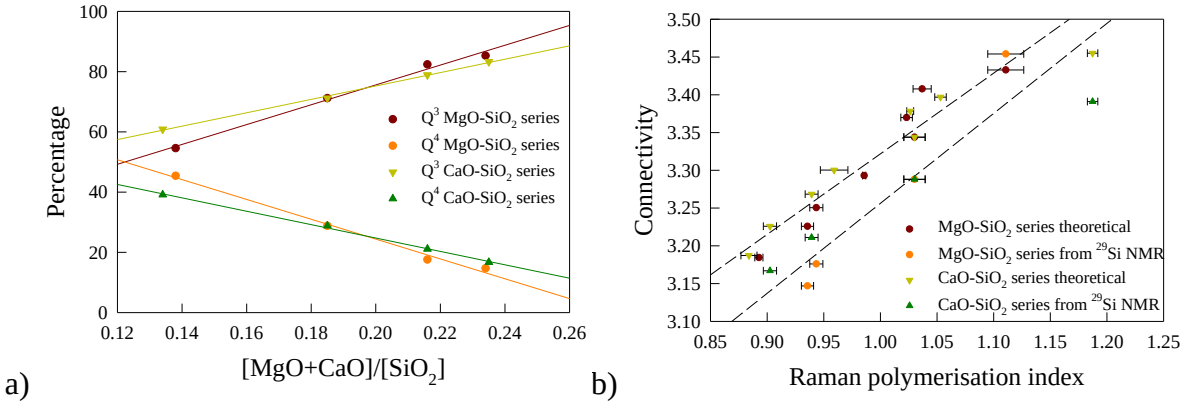

Figure 6: Glass connectivity a) Q^3 and Q^4 speciation as determined by ^{29}Si on selected samples (the solid lines are regression fits) and b) connectivity calculated from the measured composition (theoretical) and from the ^{29}Si NMR data (the dashed lines are regression fits to the data for both the $MgO\text{-}SiO_2$ and $CaO\text{-}SiO_2$ series glasses).

Figure 6a shows that the amount of Q^3 increases and Q^4 decreases as either MgO or CaO replace SiO_2 in the $MgO\text{-}SiO_2$ or $CaO\text{-}SiO_2$ series glasses. Although the structural changes are very similar in both cases, at low MgO contents the $MgO\text{-}SiO_2$ series glasses seem to be slightly more polymerised than the equivalent $CaO\text{-}SiO_2$ series glasses and vice versa for the high MgO content glasses. It can be seen from figure 6b that the connectivity as calculated from the NMR data increases with increasing Raman polymerization index, as does the connectivity calculated from the measured compositions, even though precise numerical agreement between these two approaches is not obtained. However the overall similarity in trend gives confidence that the Raman polymerization index can indeed be used to assess the network connectivity of the glasses studied here. The observed changes in the amounts of Q^4 and Q^3 species with increasing alkaline earth oxide content are consistent with the work of Jones et al[30] and Deriano et al.[6] They found that additions of CaO to a $Na_2O \cdot SiO_2$ glass reduced the amount of Q^4 whilst the amount of Q^3 increased[30] and that substitution of MgO for SiO_2 lowered the amount of Q^4 as the amount of Q^3 species increased in magnesium sodium silicate glasses[31]. This is also in agreement with Hauret et al.[32] who when comparing the imaginary dielectric function of soda-magnesia-silica and soda-lime-silica glasses found that both MgO and CaO behaved similarly as network modifiers. Although the field strength of MgO is larger than that of CaO no significant effects of cationic field strength were observed in the $MgO\text{-}SiO_2$ and $CaO\text{-}SiO_2$ series, even though such effects have been reported for alkali oxides[6,28,33]. Taken together figures 3 to 6 clearly show that modification of the

MgO-SiO_2 and CaO-SiO_2 series glasses due to either MgO or CaO substituting for SiO_2 is very similar with both species acting as modifier species. It should be noted that in both of these glass series there is always more CaO present than MgO. The data for the MgO-CaO series shown in figure 3b does indicate that there is some difference in behaviour when CaO is directly replaced by MgO resulting in glasses containing less CaO than MgO unlike what is seen in either the MgO-SiO_2 series or the CaO-SiO_2 series. In this case the MgO rich glasses do tend to have a higher Raman polymerization index, reaching the same levels as seen with highest silica contents in the other two glass series. This does suggest that MgO has a notable effect on the network forming behaviour in silicate glasses, but only if it is the dominant alkaline earth species.

3.3 Mechanical properties

Table 2 summarises the physical and mechanical data obtained for the glasses investigated here. In all three series of glasses Young's modulus, shear modulus, Poisson's ratio, bulk modulus and hardness all increase with increasing alkaline earth content and thus increase with decreasing Raman polymerisation index. Hence for the range of glasses studied here decreased network connectivity correlates with increased moduli and hardness indicating the importance of network packing for these glasses.

Table 2. Physical and mechanical properties of the glasses studied here. Glass codes are of the form $M_pC_qS_r$ where p, q and r are the batched molar contents of MgO, CaO and SiO_2 respectively. See table 1 for analysed compositions. For convenience glass $M_3C_{10}S_{72}$ appears in all 3 datasets.

Glass code	ρ /Mg m^{-3}	H_V /GPa	K_{Ic} /MPa m$^{0.5}$	Brittleness /μm$^{-1/2}$	E/ GPa	G /GPa	ν	K/ GPa	T_g /°C
$M_0C_{10}S_{75}$	2.465 ± 0.001	-	-	-	71.9 ± 0.6	29.9 ± 0.1	0.201 ± 0.005	40.1 ± 1.6	580
$M_1C_{10}S_{74}$	2.475 ± 0.001	5.46 ± 0.06	0.80 ± 0.09	6.8 ± 0.8	72.5 ± 0.6	30.0 ± 0.1	0.207 ± 0.005	41.2 ± 1.6	575
$M_2C_{10}S_{73}$	2.480 ± 0.001	5.52 ± 0.09	0.82 ± 0.06	6.7 ± 0.5	72.5 ± 0.8	30.1 ± 0.1	0.204 ± 0.006	40.8 ± 2.0	577
$M_3C_{10}S_{72}$	2.485 ± 0.001	5.63 ± 0.09	0.82 ± 0.03	6.9 ± 0.3	73.3 ± 0.4	30.3 ± 0.1	0.211 ± 0.004	42.3 ± 1.2	580
$M_4C_{10}S_{71}$	2.496 ± 0.001	5.64 ± 0.10	0.89 ± 0.08	6.3 ± 0.6	73.6 ± 0.6	30.3 ± 0.1	0.214 ± 0.005	42.9 ± 1.7	579
$M_5C_{10}S_{70}$	2.504 ± 0.001	5.72 ± 0.05	0.85 ± 0.10	6.7 ± 0.8	74.0 ± 0.7	30.4 ± 0.1	0.217 ± 0.005	43.6 ± 2.0	574
$M_6C_{10}S_{69}$	2.513 ± 0.001	5.73 ± 0.06	0.88 ± 0.05	6.5 ± 0.3	74.0 ± 0.8	30.5 ± 0.1	0.213 ± 0.006	43.0 ± 2.2	580
$M_7C_{10}S_{68}$	2.520 ± 0.001	5.96 ± 0.08	0.80 ± 0.09	7.4 ± 0.8	75.6 ± 0.7	31.1 ± 0.1	0.214 ± 0.005	44.1 ± 1.9	575
$M_3C_7S_{75}$	2.445 ± 0.001	-	-	-	71.8 ± 0.6	30.0 ± 0.1	0.197 ± 0.005	39.5 ± 1.5	563

$M_3C_8S_{74}$	2.462 ± 0.001	5.37 ± 0.08	0.78 ± 0.06	6.9 ± 0.6	72.0 ± 0.7	30.0 ± 0.1	0.199 ± 0.006	39.8 ± 1.7	578
$M_3C_9S_{73}$	2.474 ± 0.001	5.50 ± 0.05	0.83 ± 0.09	6.6 ± 0.7	72.7 ± 0.7	30.3 ± 0.1	0.201 ± 0.006	40.6 ± 1.7	583
$M_3C_{10}S_{72}$	2.485 ± 0.001	5.63 ± 0.09	0.82 ± 0.03	6.9 ± 0.3	73.3 ± 0.4	30.3 ± 0.1	0.211 ± 0.004	42.3 ± 1.2	580
$M_3C_{11}S_{71}$	2.504 ± 0.001	5.65 ± 0.05	0.89 ± 0.05	6.4 ± 0.4	74.0 ± 0.7	30.5 ± 0.1	0.213 ± 0.006	42.9 ± 1.9	584
$M_3C_{12}S_{70}$	2.508 ± 0.001	5.69 ± 0.08	0.90 ± 0.05	6.3 ± 0.4	73.8 ± 0.5	30.3 ± 0.1	0.217 ± 0.005	43.4 ± 1.5	582
$M_3C_{13}S_{69}$	2.529 ± 0.001	5.69 ± 0.08	0.86 ± 0.06	6.6 ± 0.5	74.9 ± 1.0	31.0 ± 0.1	0.207 ± 0.005	42.7 ± 2.5	572
$M_3C_{14}S_{68}$	2.542 ± 0.001	5.81 ± 0.03	0.95 ± 0.03	6.1 ± 0.2	75.6 ± 0.9	31.2 ± 0.1	0.213 ± 0.005	43.9 ± 2.4	573
$M_1C_{12}S_{72}$	2.502 ± 0.001	5.39 ± 0.01	0.86 ± 0.03	6.0 ± 0.2	73.7 ± 0.6	30.4 ± 0.1	0.211 ± 0.003	42.5 ± 1.5	574
$M_3C_{10}S_{72}$	2.485 ± 0.001	5.63 ± 0.09	0.82 ± 0.01	6.3 ± 0.1	73.3 ± 0.5	30.3 ± 0.1	0.211 ± 0.002	42.3 ± 1.2	571
$M_5C_8S_{72}$	2.469 ± 0.001	5.33 ± 0.01	0.73 ± 0.01	7.2 ± 0.1	73.2 ± 0.9	30.3 ± 0.1	0.207 ± 0.004	41.6 ± 2.3	551
$M_7C_6S_{72}$	2.457 ± 0.001	5.25 ± 0.02	0.78 ± 0.05	6.9 ± 0.5	72.8 ± 0.9	30.4 ± 0.1	0.199 ± 0.004	40.3 ± 2.2	556
$M_9C_4S_{72}$	2.446 ± 0.003	5.21 ± 0.01	0.76 ± 0.02	7.4 ± 0.2	71.4 ± 0.9	29.6 ± 0.1	0.205 ± 0.004	40.3 ± 2.3	558
$M_{11}C_2S_{72}$	2.433 ± 0.001	5.16 ± 0.02	0.78 ± 0.06	6.9 ± 0.6	70.7 ± 0.9	29.4 ± 0.1	0.203 ± 0.004	39.6 ± 2.2	561

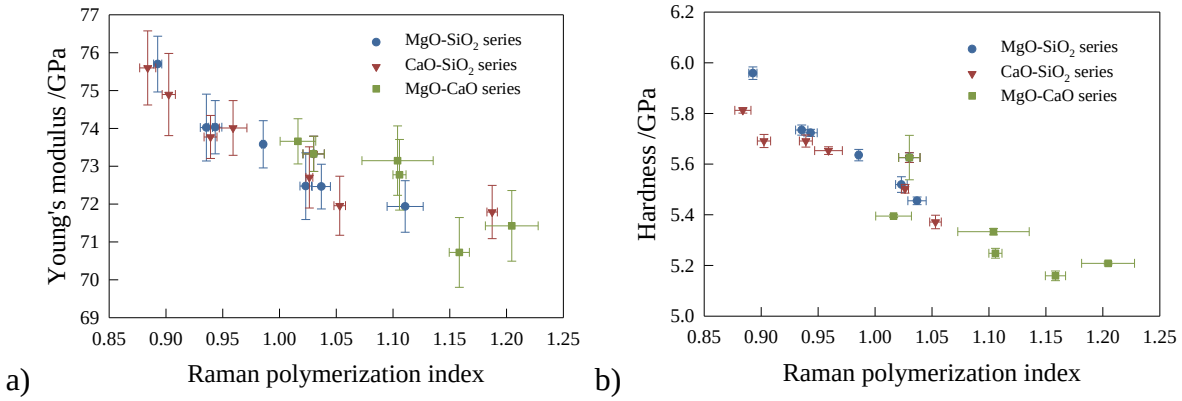

Figure 7: Variation of selected mechanical properties with Raman polymerization index for all 3 series of glasses studied here: a) Young's modulus and b) hardness

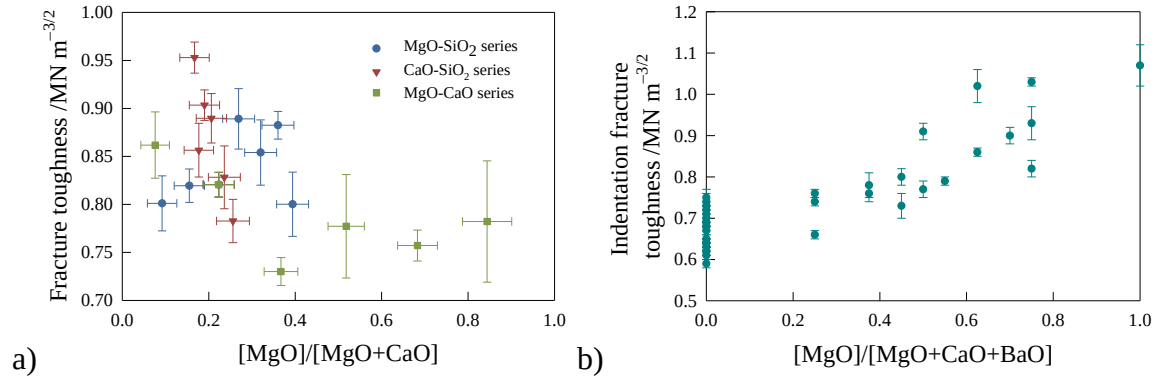

Figure 8: a) Variation of plane strain fracture toughness with MgO fraction and b) variation of indentation fracture toughness with MgO fraction taken from Hand & Tadjiev[2]

From tables 1 and 2 it is clear that there is no simple correlation between the changes in the observed properties and the magnesia content as a fraction of the total alkaline earth content in contrast to the earlier reports of Deriano et al.[6] and Hand & Tadjiev[2]. Figure 8 compares the fracture toughness behaviour as a function of [MgO]/Σ[RO] for the current study (figure 8a) and the data taken from Hand and Tadjiev (figure 8b). Inasmuch as figure 8a shows any sort of trend it appears that fracture toughness may be decreasing with increasing magnesia content which is the opposite behaviour seen in figure 8b. It should be noted that Hand and Tadjiev measured indentation fracture toughness, rather than using a bend test with a controlled defect to measure fracture toughness as is the case here. Although indentation has been widely used as a convenient method for measuring fracture toughness of brittle materials in general and glasses in particular (see, for example, Barlet et al.[34], Hasdemir et al.[31]) its validity has been significantly questioned[35] and the opposing trends seen in figures 8a and 8b raises further questions about the validity of the approach.

From figure 8a and table it can seen that the variations in fracture toughness are quite significant. The lowest fracture toughness value is 0.73 MN $m^{-3/2}$ (for glass $M_5C_8S_{72}$) and the highest is 0.95 MN $m^{-3/2}$ (for glass $M_3C_{14}S_{68}$). Thus the highest fracture toughness was obtained from the composition with the largest amount of lime but lowest amount of silica. It is also notable from the figure that the fracture toughness drops quite rapidly with decreasing CaO content. Meanwhile there is relatively little variation in fracture toughness for the high magnesia glasses although the error bars are larger in this region. Thus for conventional soda-lime-silica glasses (on which the current compositions are all based) there would appear to be some benefit in increasing lime at the expense of silica to obtain higher fracture toughness values.

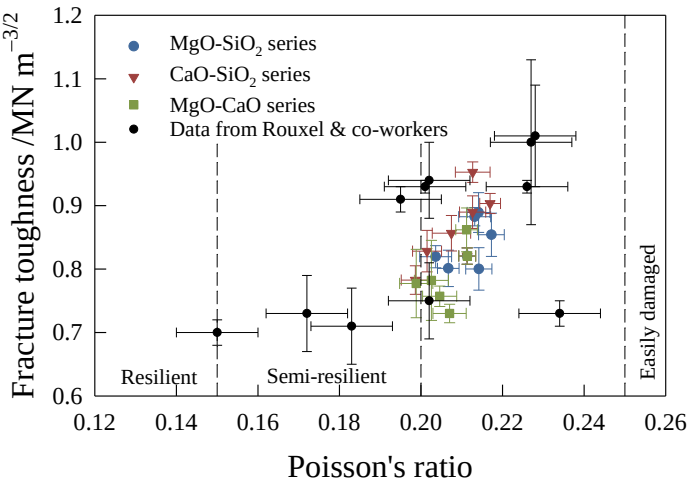

Figure 9: Fracture toughness versus Poisson's ratio for all 3 series of glasses studied here along with data taken from Rouxel & co-workers[6,38,39]

Recently Rouxel and co-workers[36,37] have looked at how the damage arising from indentation behaviour changes with Poisson's ratio. Using their definitions concerning the ease of corner cracking around indentations the glasses studied here essentially fall into the semi-resilient glass category ($0.20 < \nu < 0.25$), although the lowest alkaline earth glasses tend to just fall into resilient glass category ($0.15 < \nu < 0.20$). The data in table 2 suggests that fracture toughness tends to increase as Poisson's ratio increases although the correlation is not very strong. When this data is plotted along with bend test fracture toughness data published by Rouxel and co-workers[38,39] this correlation is more obvious although one point (which corresponds to a glass with a higher packing density) indicates other factor may be important. However combining these results does indicate that resistance to cracking arising from contact damage may tend to correlate with lower rather than higher fracture toughness. Thus glasses that are more resistant to crack growth from a pre-existing defect may actually be easier to damage. This is because glasses with lower packing densities tend to have lower Poisson's ratios (although for the glasses studied here Poisson's ratio is not strongly correlated with packing density as they fall into the near vertical part of the correlation found by Rouxel[10]) and thus they can densify more easily giving rise to better contact resistance. However this does still raise the issue of whether it is better to have a glass that is more resilient to contact damage, therefore presumably making it more difficult to create a strength controlling defect, or for the glass to be more resistant to fast fracture once some damage has occurred?

4. Conclusions

For the MgO-SiO_2 series and CaO-SiO_2 glasses increasing the alkaline earth content at the expense of the silica content resulted in increased network depolymerisation, whereas for the MgO-CaO series when MgO became the dominant alkaline earth species, network depolymerisation was reduced. It was also found that the moduli and hardness reduced as the network became more depolymerised. Thus while MgO and CaO both act as network modifiers when more CaO than MgO is present in soda-lime-silica glasses, as one moves towards magnesia rich soda-magnesia-silica glasses with a low lime content a difference in behaviour is observed. However, in contradiction to previous data no significant advantage of replacing CaO by MgO was found. In the case of the fracture toughness measurements this may be associated with the fact that bend testing rather than indentation testing has been used here; it is appears that the glasses with the lowest fracture toughness values may be more resilient to contact damage than those with the higher fracture toughness values.

Acknowledgements

EK thanks Gurallar Artcraft for funding. We thank David Apperley of the UK National NMR Facility at Durham for providing the NMR data. We thank Glass Technology Services for the XRF measurements.

Appendix

For the single edge notch bend test Y_{max} is greater value of either Y_s or Y_d which are given by

$$Y_d = \left(\sqrt{\pi} M H_2\right) / \sqrt{Q} \tag{A1}$$

$$Y_S = \left(\sqrt{\pi} M S H_1\right) / \sqrt{Q} \tag{A2}$$

where

$$Q = 1 + 1.464(a/c)^{1.65} \tag{A3}$$

$$M = \left[1.13 - 0.09\left(\frac{a}{c}\right)\right] + \left\{-0.54 + \frac{0.89}{0.2 + a/c}\right\}\left(\frac{a}{W}\right)^2 + \left\{0.5 - \frac{1}{0.65 + a/c} + 14\left(1 - \frac{a}{c}\right)^{24}\right\}\left(\frac{a}{W}\right)^4 \quad \text{(A4)}$$

$$S = \left[1.1 + 0.35\left(\frac{a}{W}\right)^2\right]\sqrt{\frac{a}{c}} \quad \text{(A5)}$$

$$H_1 = 1 - \left[0.34 + 0.11\left(\frac{a}{c}\right)\right]\left(\frac{a}{W}\right) \quad \text{(A6)}$$

$$H_2 = 1 - \left[1.22 + 0.12\left(\frac{a}{c}\right)\right]\left(\frac{a}{W}\right) + \left[0.55 - 1.05\left(\frac{a}{c}\right)^{0.75} + \left(\frac{a}{c}\right)^{1.5}\right]\left(\frac{a}{W}\right)^2 \quad \text{(A7)}$$

where a and c are the crack depth and half surface crack length and W is the specimen depth.

References

1 J. Sehgal & S. Ito, J. Non-Cryst. Solids **253** (1999) 126-132
2 R.J. Hand & D.R. Tadjiev, J. Non-Cryst. Solids **356** (2010) 2417–2423
3 H.A Schaeffer, Solid State Ionics **105** (1998) 265-270
4 J. Sehgal & S. Ito J. Am. Ceram. Soc., **81** (1998) 2485–88 (1998)
5 J.G.R. Kingston & R.J. Hand Fatig. Fract. Engng. Mater. Structs. **23** (2000) 685-690
6 S. Deriano, T. Rouxel, M. LeFloch & B. Beuneu Phys. Chem. Glasses **45** (2004) 37-44
7 A. Mohajerani & J.W. Zwanziger J. Non-Cryst. Solids **358** (2012) 1474-1479
8 A. Makashima and J.D. Mackenzie J. Non-Cryst. Solids **12** (1973) 35-45
9 A. Makashima and J.D. Mackenzie J. Non-Cryst. Solids **17** (1975) 147-157
10 T. Rouxel J. Amer. Ceram. Soc. **90** (2007) 3019-3039
11 A. Pedone, G. Malavasi, M.C. Menziani, U. Segre & A.N. Cormack, J. Phys. Chem. **112** (2008) 11034-11041
12 Ph. Columban, A. Tournie & L. Bellot-Gurlet J. Raman Spectrosc. **37** (2006) 841-852
13 BS EN ISO 18756: 2005
14 G.S. Glaesemann, J.E. Ritter & K. Jakus, J. Amer. Ceram. Soc. **70** (1987) 630-636
15 M. Yoda, Engng. Fract. Mech. **28** (1987) 77-84
16 R. Samuel, S. Chandrasekar, T.N. Farris & R.H. Licht, J. Amer. Ceram. Soc. **72** (1989)
17 G.D. Quinn & J.A. Salem, J. Amer. Ceram. Soc. **85** (2002) 873-880
18 C. Le Losq, D.R. Neuville, P. Florian, G.S. Henderson and D. Massiot Geochim. Cosmochim. Acta, **126** (2014) 495-517
19 P. Columban and O. Paulson J. Amer. Ceram. Soc. **88** (2005) 390-395
20 G.S. Henderson, G.M. Bancroft, M.E. Fleet & D.J. Rogers, Amer. Min, **70** (1985) 946-960

[21] T. Furukawa, K.E. Fox & W.B. White, J. Chem. Phys. **75** (1981) 3226-3237
[22] P.F. McMillan, Ann. Rev. Earth Planet. Sci. **17** (1989) 255-283
[23] D.W. Matson, S.K. Sharma & J.A. Philpotts J. Non-Cryst. Solids **58** (1983) 323-325
[24] P. McMillan Amer. Min. **69** (1984) 622-644
[25] T. Tsujimura, XY Xue, M. Kanzaki and M.J. Walter, Geochim. Cosmochim. Acta, **68** (2004) 5081-5101
[26] Ph. Colomban, J. Non-Cryst. Solids **323** (2003) 180-187
[27] Ph. Colomban, M-P. Etcheverry, M. Asquier, M. Bounichou & A. Tournié J. Raman Spectro. **37** (2006) 614-626
[28] H. Maekawa, T. Maekawa, K. Kawamura & T. Yokokawa, J. Non-Cryst. Solids **127** (1991) 53-64
[29] R. Dupree, D. Holland, P.W. McMillan & R.F. Pettifer, J. Non-Cryst. Solis **68** (1984) 399-410
[30] A.R. Jones, R. Winter, G.N. Greaves & I.H. Smith J. Non-Cryst. Solids **293-295 (**2001) 87-92
[31] I. Hasdemir, S. Striepe, J. Deubener and K. Simon, J. Non-Cryst. Solids, **408** (2015) 51–56
[32] G. Hauret, Y. Vaills, Y. Luspin, F. Gervais & B. Coté, J. Non-Cryst. Solids **170** (1994) 175-181
[33] J.B. Murdoch, J.F. Stebbins & I.S.E. Carmichael, Amer. Min. **70** (1995) 332-343
[34] M. Barlet, J-M. Delaye, T. Charpentier, M. Gennisson, D. Bonamy, T. Rouxel & C.L. Rountree, J. Non-Cryst. Solids **417–418** (2015) 66–79
[35] G.D. Quinn and R.C. Bradt, J. Amer. Ceram. Soc. **90** (2000) 673-680
[36] T. Rouxel, H. Ji, J.P. Guin, F. Augereau & B. Rufflé, J. Appl. Phys. **107** (2010) 094903
[37] T. Rouxel, P. Sellappan, F. Célarié, P. Houizot, J-C. Sangleboeuf, C. R.Mecanique **342** (2014) 46–51
[38] S. Dériano, A. Jarry , T. Rouxel, J.-C. Sangleboeuf & S. Hampshire, J. Non-Cryst. Solids, **344** (2004) 44-50
[39] P. Sellappan, T. Rouxel, F. Celarie, E. Becker, P. Houizot & R. Conradt, Acta Mater., **61** (2013) 5949–5965